A Novel ZF and MMSE Receiver for Modified Walsh-Hadamard Code Division Multiplexing in Helicopter Satellite Communications

Toshiharu Kojima and Tsubasa Yamada
Department of Computer and Network Engineering, Graduate School of Informatics and Engineering,
The University of Electro-Communications, 1-5-1 Chofugaoka, Chofu, Tokyo, 182-8585, Japan
Email: {Kojima.Toshiharu@, y2031153@edu.cc.}uec.ac.jp

***Abstract*—In helicopter satellite communications, overcoming periodic signal blockage caused by rotor blades is an important issue. Modified Walsh-Hadamard code division multiplexing (MWHCDM) is a promising solution. However, it is adversely affected by the inter-code interference (ICI) due to the periodic blockage. This paper proposes an ICI reduction scheme for MWHCDM. The proposed one utilizes the structure of the MWHCDM signal for reducing the ICI with zero-forcing (ZF) and minimum mean square error (MMSE) detection. The results of computer simulation demonstrated that the proposed one achieves both excellent bit error rate performance and superior spectral efficiency in the periodic blockage channel.**

I. Introduction

Helicopters are indispensable to emergency rescue, disaster relief, and video transmission of disaster situations. Undisputedly, communication between the base station and the helicopter is important in these missions. Helicopter satellite communications, which provide reliable communication regardless of landform, have to combat the periodic blockage of the transmission channel due to rotor blades [1]–[7]. Walsh-Hadamard (WH) code division multiplexing (CDM) [2] is attractive as it overcomes the periodic blockage with an implicit time diversity effect.

The bit error rate (BER) performance of WHCDM in the periodic blockage channel is improved by reducing the inter-code interference (ICI) caused by the periodic blockage. Although the explicit time diversity (ETD) is effective to reduce the ICI [2], it degrades the spectral efficiency. In [4], a low ICI WHCDM was proposed. We call it modified WHCDM (MWHCDM). Without using ETD, MWHCDM achieves the same BER performance as WHCDM with ETD (ETD-WHCDM). That is, MWHCDM is superior to ETD-WHCDM in terms of spectral efficiency [4]. As further ICI reduction methods, applying maximal ratio combining (MRC), zero-forcing (ZF), and minimum mean square error (MMSE) detection to ETD-WHCDM was investigated, and it was shown that ZF and MMSE detection improve the BER performance more [5].

It is expected that the BER performance of MWHCDM is also enhanced with ZF and MMSE detection. In the periodic blockage channel, however, ZF and MMSE detection require ETD because of zero channel gain. Introducing ETD means that MWHCDM loses the advantage in spectral efficiency. To solve this dilemma, we propose a ZF and MMSE detection scheme using no ETD for MWHCDM in this paper. The proposed scheme utilizes the structure inherent in MWHCDM symbols for performing ZF and MMSE detection without ETD. The results of computer simulation showed that the BER performance of the proposed one is close to the theoretical lower bound in the periodic blockage channel, and is identical with that of ETD-WHCDM employing ZF and MMSE detection. In other words, the proposed scheme achieves both excellent BER performance and superior spectral efficiency.

The rest of the paper is organized as follows: Section II and III describe the conventional and proposed scheme, respectively. In Section IV, we evaluate the BER performance of the proposed one by computer simulation. Finally, we conclude the paper in Section V.

II. Conventional scheme

Figures 1 and 2 illustrate the configuration of the transmitter and conventional receiver of MWHCDM [4], respectively. The primary modulation of MWHCDM is binary phase-shift keying (BPSK). The multiplexing and demultiplexing of (M)WHCDM are mathematically described as WH transform (WHT). Let N denote the multiplexing factor.

A. Transmitter

In Fig. 1, the binary information data $a_i \in \{0, 1\}$ is input to the BPSK modulator, resulting in the following primary modulated signal b_i:

$$b_i = \sqrt{E_b} \cos a_i \pi \tag{1}$$

where E_b is the signal energy per bit. The MWHCDM symbol $\boldsymbol{S}$ is produced with the WHT processor as follows:

$$\boldsymbol{S} = \frac{1}{\sqrt{N}} \boldsymbol{H}_N \begin{bmatrix} \boldsymbol{B}_0 \\ j\boldsymbol{B}_1 \end{bmatrix} \tag{2}$$

where $\boldsymbol{H}_N$ is the WH matrix of order N, and

$$\boldsymbol{B}_0 = \begin{bmatrix} b_1 & b_2 & \cdots & b_{N/2} \end{bmatrix}^{\mathrm{T}} \tag{3}$$

$$\boldsymbol{B}_1 = \begin{bmatrix} b_{N/2+1} & b_{N/2+2} & \cdots & b_N \end{bmatrix}^{\mathrm{T}} \tag{4}$$

are the primary modulated symbols formed by the serial-to-parallel converter (S/P). Let s_i denote the i-th element of $\boldsymbol{S}$. Each s_i is sent to the channel as the i-th transmitted signal through the parallel-to-serial converter (P/S).

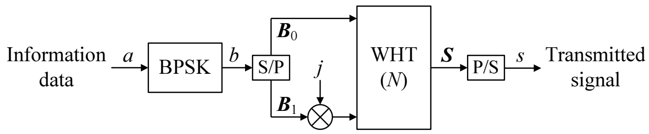

Fig. 1. Configuration of the transmitter.

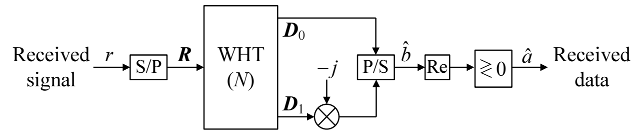

Fig. 2. Configuration of the conventional receiver.

B. Receiver

Letting the i-th received signal be denoted by r_i, the received symbol $\boldsymbol{R}$ in Fig. 2 is represented as

$$\boldsymbol{R} = \begin{bmatrix} r_1 & r_2 & \cdots & r_N \end{bmatrix}^{\mathrm{T}}. \tag{5}$$

The WHT processor transforms the received symbol $\boldsymbol{R}$ into the demultiplexed symbols $\boldsymbol{D}_0$ and $\boldsymbol{D}_1$ corresponding to $\boldsymbol{B}_0$ and $j\boldsymbol{B}_1$ in the transmitter, respectively. This processing is expressed by the following equation:

$$\begin{bmatrix} \boldsymbol{D}_0 \\ \boldsymbol{D}_1 \end{bmatrix} = \frac{1}{\sqrt{N}} \boldsymbol{H}_N \boldsymbol{R}. \tag{6}$$

Let $\hat{b}_i$ denote the i-th element of the following final processed symbol $\hat{\boldsymbol{B}}$:

$$\hat{\boldsymbol{B}} = \begin{bmatrix} \boldsymbol{D}_0 \\ -j\boldsymbol{D}_1 \end{bmatrix}. \tag{7}$$

On the basis of whether the real part of $\hat{b}_i$ is positive or negative, the received data $\hat{a}_i \in \{0, 1\}$ is decided.

III. Proposed scheme

A. Characteristics of MWHCDM symbols

The WH matrix has the following structure:

$$\boldsymbol{H}_N = \begin{bmatrix} \boldsymbol{H}_{N/2} & \boldsymbol{H}_{N/2} \\ \boldsymbol{H}_{N/2} & -\boldsymbol{H}_{N/2} \end{bmatrix}. \tag{8}$$

Substituting (8) into (2) yields

$$\boldsymbol{S} = \frac{1}{\sqrt{N}} \begin{bmatrix} \boldsymbol{H}_{N/2}(\boldsymbol{B}_0 + j\boldsymbol{B}_1) \\ \boldsymbol{H}_{N/2}(\boldsymbol{B}_0 - j\boldsymbol{B}_1) \end{bmatrix} = \begin{bmatrix} \boldsymbol{S}_0 \\ \boldsymbol{S}_1 \end{bmatrix} \tag{9}$$

where

$$\boldsymbol{S}_0 = \frac{1}{\sqrt{2}} \frac{1}{\sqrt{N/2}} \boldsymbol{H}_{N/2}(\boldsymbol{B}_0 + j\boldsymbol{B}_1) \tag{10}$$

$$\boldsymbol{S}_1 = \frac{1}{\sqrt{2}} \frac{1}{\sqrt{N/2}} \boldsymbol{H}_{N/2}(\boldsymbol{B}_0 - j\boldsymbol{B}_1). \tag{11}$$

From (10), (11) and the fact that the primary modulated signal b_i is real as shown in (1), we have

$$\boldsymbol{S}_1{}^* = \boldsymbol{S}_0 \tag{12}$$

where $*$ denotes the complex conjugate. Equations (10) and (11) also show that $\boldsymbol{S}_0$ and $\boldsymbol{S}_1$ are WHCDM symbols of the multiplexing factor $N/2$ with half energy. Hence, the concatenation of $\boldsymbol{S}_0$ and $\boldsymbol{S}_1{}^*$ is identical to a pair of the ETD-WHCDM symbols. Letting $\boldsymbol{R}_0$ and $\boldsymbol{R}_1$ denote the first and second half of the received symbol $\boldsymbol{R}$, respectively, $\boldsymbol{R}_0$ and $\boldsymbol{R}_1{}^*$ also constitute the pair of the ETD-WHCDM symbols. This allows the proposed scheme to perform ZF and MMSE detection in the periodic blockage channel without using ETD.

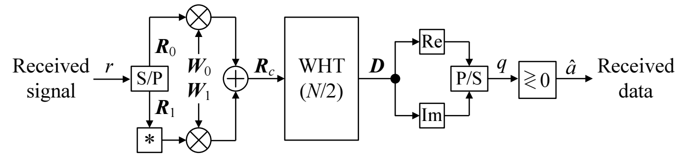

Fig. 3. Configuration of the proposed receiver.

B. Configuration of the proposed scheme

As the proposed scheme concerns ZF and MMSE detection, the transmitter is the same as shown in Fig. 1. The configuration of the proposed receiver is depicted in Fig. 3. In the proposed receiver, the received symbol $\boldsymbol{R}$ is divided into the following $\boldsymbol{R}_0$ and $\boldsymbol{R}_1$:

$$\boldsymbol{R}_0 = \begin{bmatrix} r_1 & r_2 & \cdots & r_{N/2} \end{bmatrix}^{\mathrm{T}} \tag{13}$$

$$\boldsymbol{R}_1 = \begin{bmatrix} r_{N/2+1} & r_{N/2+2} & \cdots & r_N \end{bmatrix}^{\mathrm{T}}. \tag{14}$$

The combined symbol $\boldsymbol{R}_c$ is given as

$$\boldsymbol{R}_c = \begin{bmatrix} \boldsymbol{W}_0 & \boldsymbol{W}_1 \end{bmatrix} \begin{bmatrix} \boldsymbol{R}_0 \\ \boldsymbol{R}_1{}^* \end{bmatrix} \tag{15}$$

where

$$\boldsymbol{W}_0 = \mathrm{diag}\left(w_1^0,\, w_2^0,\, \cdots,\, w_{N/2}^0\right) \tag{16}$$

$$\boldsymbol{W}_1 = \mathrm{diag}\left(w_1^1,\, w_2^1,\, \cdots,\, w_{N/2}^1\right) \tag{17}$$

are the weighting matrices consisting of the weighting factors w_i^0 and w_i^1, respectively. The WHT processor of order $N/2$ outputs the following demultiplexed symbol $\boldsymbol{D}$:

$$\boldsymbol{D} = \frac{1}{\sqrt{N/2}} \boldsymbol{H}_{N/2} \boldsymbol{R}_c. \tag{18}$$

Comparing (6) with (18) shows that the proposed scheme reduces the computational complexity of WHT in demultiplexing. As the combined symbol $\boldsymbol{R}_c$ corresponds to $\boldsymbol{S}_0$ in (10), the demultiplexed symbol $\boldsymbol{D}$ is similarly corresponding to $\boldsymbol{B}_0 + j\boldsymbol{B}_1$. Thus the received data $\hat{a}_i$ is decided as follows:

$$\hat{a}_i = \begin{cases} 0 & (q_i \geq 0) \\ 1 & (q_i < 0) \end{cases} \tag{19}$$

where

$$q_i = \begin{cases} \mathrm{Re}[d_i] & (1 \leq i \leq N/2) \\ \mathrm{Im}[d_{i-N/2}] & (N/2+1 \leq i \leq N) \end{cases} \tag{20}$$

and d_i is the i-th element of the demultiplexed symbol $\boldsymbol{D}$.

C. Derivation of weighting factors

From (13)–(17), the i-th element r_{ci} of the combined symbol $\boldsymbol{R}_c$ is expressed by

$$r_{ci} = w_i^0 r_i + w_i^1 {r_{N/2+i}}^*. \tag{21}$$

In a frequency non-selecting channel including the periodic blockage channel, the received signal r_i is described as

$$r_i = h_i s_i + n_i \tag{22}$$

where h_i denotes the channel gain and n_i is additive white Gaussian noise (AWGN). Additionally, the characteristics of the MWHCDM symbol shown in (12) is equivalent to the following equation:

$${s_{N/2+i}}^* = s_i. \tag{23}$$

From (21)–(23), we have

$$r_{ci} = \left(w_i^0 h_i + w_i^1 {h_{N/2+i}}^*\right) s_i + w_i^0 n_i + w_i^1 {n_{N/2+i}}^*. \tag{24}$$

This equation shows that the proposed scheme performs the equal-gain combining (EGC) when $w_i^0 = w_i^1 = 1$, i.e., both $\boldsymbol{W}_0$ and $\boldsymbol{W}_1$ are the identity matrices of order $N/2$. Clearly, the BER performance of EGC is the same as that of the conventional scheme.

In the following, we derive the weighting factors to perform ZF and MMSE detection. Equation (24) shows that the ZF weighting factors should satisfy the following equation:

$$w_i^0 h_i + w_i^1 {h_{N/2+i}}^* = 1. \tag{25}$$

In addition, to maximize the signal-to-noise power ratio, we apply MRC. That is,

$$w_i^0 = \gamma {h_i}^* \tag{26}$$
$$w_i^1 = \gamma h_{N/2+i} \tag{27}$$

where γ is a non-zero constant. From (25)–(27), we obtain the ZF weighting factors as follows:

$$w_i^0 = \frac{{h_i}^*}{|h_i|^2 + |h_{N/2+i}|^2} \tag{28}$$
$$w_i^1 = \frac{h_{N/2+i}}{|h_i|^2 + |h_{N/2+i}|^2}. \tag{29}$$

The condition of MMSE detection is described by the following equation:

$$\frac{\partial}{\partial w_i^k} \mathrm{E}\left[|r_{ci} - s_i|^2\right] = 0 \quad (k = 0, 1). \tag{30}$$

Letting N_0 be the one-sided power spectral density of AWGN, solving (30) yields the following MMSE weighting factors:

$$w_i^0 = \frac{{h_i}^*}{|h_i|^2 + |h_{N/2+i}|^2 + (E_b/N_0)^{-1}} \tag{31}$$
$$w_i^1 = \frac{h_{N/2+i}}{|h_i|^2 + |h_{N/2+i}|^2 + (E_b/N_0)^{-1}}. \tag{32}$$

Note that ZF and MMSE detection in the periodic blockage channel is executable unless h_i and $h_{N/2+i}$ are zero, i.e., both s_i and $s_{N/2+i}$ are blocked.

TABLE I
SIMULATION CONDITIONS

Primary modulation	BPSK
Transmission data rate	64 kbps
Multiplexing factor N	2048 (uncoded), 4096 (coded)
Forward error correction	Convolutional coding with Viterbi decoding
Coding rate	1/2
Constraint length	7
Blockage period	38.9 msec
Blockage ratio ρ	0.086 (typical), 0.321 (worst)

IV. Computer simulation

A. Channel model and simulation conditions

In the simulation, as a model of the periodic blockage with the period T_p, we use the following $h(t)$:

$$h(t) = \prod_{k=-\infty}^{\infty} u(t - kT_p) \tag{33}$$

where

$$u(t) = \begin{cases} 0 & (0 \le t < T_d) \\ 1 & (\text{otherwise}) \end{cases} \tag{34}$$

is a single blockage of the duration T_d. Letting T_c denote the chip duration, the channel gain h_i is given by $h_i = h(iT_c)$. We define the blockage ratio ρ as T_d/T_p.

The simulation conditions are summarized in Table I. We compare the uncoded BER performance of the proposed scheme with that of the conventional one. The loss of the signal energy due to the periodic blockage is ρE_b per bit on average. As the primary modulation of MWHCDM is BPSK, the following P_b gives the lower bound on the uncoded BER in the periodic blockage channel:

$$P_b = \frac{1}{2} \operatorname{erfc} \sqrt{\frac{(1-\rho)E_b}{N_0}}. \tag{35}$$

If we completely remove the ICI, the lower bound P_b is achievable. In addition, we compare the proposed one with ETD-WHCDM of the diversity factor 2 in terms of the coded BER performance.

B. Comparison with conventional scheme

Figures 4 and 5 show the uncoded BER performance under $\rho = 0.086$ and 0.321, respectively. The proposed scheme significantly outperforms the conventional one, and its BER performance is close to the lower bound. ZF and MMSE detection achieve almost the same performance. The difference in E_b/N_0 from the lower bound is about 0.3 and 0.6 dB under $\rho = 0.086$ and 0.321, respectively. This suggests that both ZF and MMSE detection almost remove the ICI.

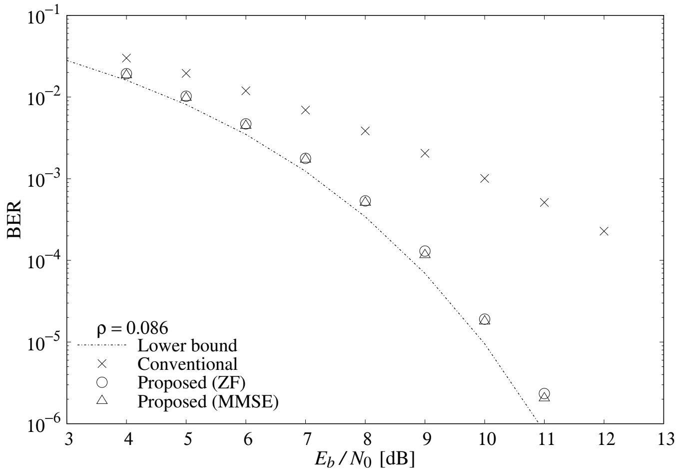

Fig. 4. Uncoded BER performance under $\rho = 0.086$.

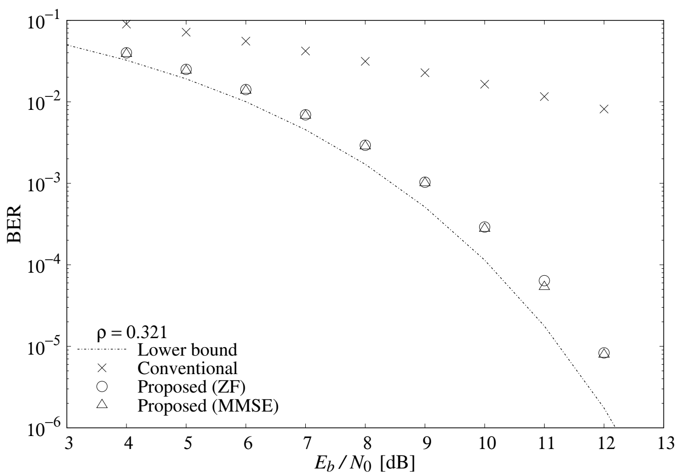

Fig. 5. Uncoded BER performance under $\rho = 0.321$.

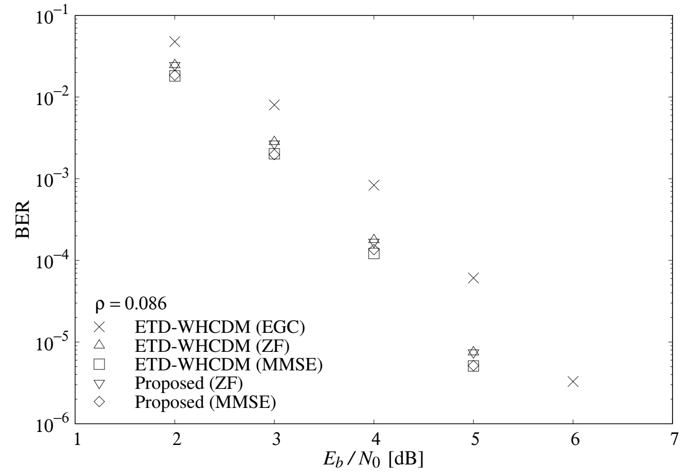

Fig. 6. Coded BER performance under $\rho = 0.086$.

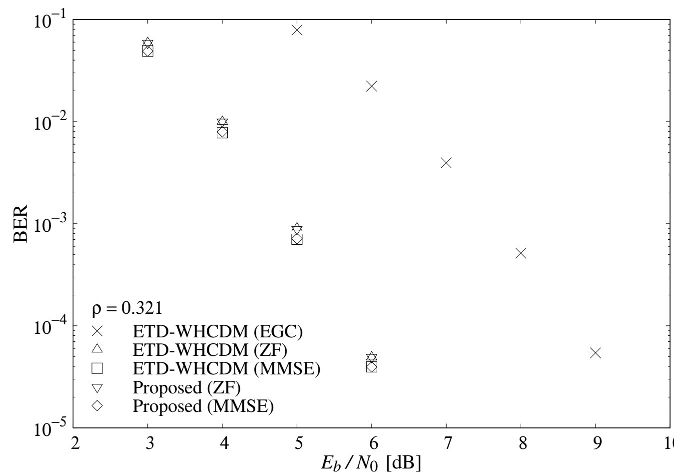

Fig. 7. Coded BER performance under $\rho = 0.321$.

C. Comparison with ETD-WHCDM

Figures 6 and 7 compare the coded BER performance of the proposed scheme with that of ETD-WHCDM under $\rho =$ 0.086 and 0.321, respectively. The proposed one achieves the same BER performance as the corresponding ETD-WHCDM. MMSE detection slightly outperforms ZF detection. As the diversity factor of ETD-WHCDM is 2, the chip rate of the proposed one is half as that of ETD-WHCDM. Therefore, the proposed one is superior in terms of spectral efficiency. Moreover, the proposed one improves the BER performance of ETD-WHCDM with EGC, which is identical to that of the conventional one. Remarkably, the improvement in E_b/N_0 is 3 dB at BER $= 10^{-4}$ under $\rho = 0.321$, i.e., the worst condition.

V. Conclusion

We have proposed a novel ICI reduction scheme for MWHCDM. The proposed one performs ZF and MMSE detection without ETD in the periodic blockage channel. The results of computer simulation demonstrated that the proposed one achieves both excellent BER performance and superior spectral efficiency. Therefore, we conclude that the proposed one is promising in helicopter satellite communications.

References

[1] E. Lemos, M. García, A. Vazquez, and S. García, "Measurement, characterization, and modeling of the helicopter satellite communication radio channel," *IEEE Trans. Antennas Propag.*, July 2014, vol. 62, no. 7, pp. 3776–3785.

[2] T. Kojima and S. Fujiwara, "Performance of Walsh-Hadamard code division multiplexing in helicopter satellite communications," in *Proc. ATC 2015*, Ho Chi Minh City, Vietnam, Oct. 2015, pp. 662–665.

[3] P. Wang, L. Yin and J. Lu, "Efficient helicopter–satellite communication scheme based on check-hybrid LDPC coding," *Tsinghua Sci. Technol.*, June 2018, vol. 23, no. 3, pp. 323–332.

[4] T. Kojima and G. Muto, "A low inter-code interference Walsh-Hadamard code division multiplexing for helicopter satellite communications," in *Proc. ATC 2018*, Ho Chi Minh City, Vietnam, Oct. 2018, pp. 1–4.

[5] G. Muto and T. Kojima, "Inter-code interference reduction in Walsh-Hadamard code division multiplexing for helicopter satellite communications," in *Proc. ATC 2019*, Hanoi, Vietnam, Oct. 2019, pp. 19–22.

[6] Y. Huang and S. Zhai, "A carrier tracking technology under helicopter rotor occlusion," in *Proc. ICCC 2019*, Chengdu, China, Dec. 2019, pp. 1069–1074.

[7] H. Jia, Z. Ni, L. Kuang, and J. Lu, "Joint occlusion detection and phase estimation algorithm for helicopter satellite communication," *IEEE Trans. Aero. Elec. Sys.*, Feb. 2020, vol. 56, no. 1, pp. 687–697.